Antiviral Research 92 (2011) 415–423

Contents lists available at SciVerse ScienceDirect

Antiviral Research

journal homepage: www.elsevier.com/locate/antiviral

HIV protease inhibitors induce metabolic dysfunction in part via increased JNK1/2 pro-inflammatory signaling in L6 cells

Lindsey D. Bogachus [a,b], Lorraine P. Turcotte [a,b,*]

[a] Department of Biological Sciences, Dana and David Dornsife College of Letters, Arts and Sciences, University of Southern California, Los Angeles, CA, United States
[b] Department of Kinesiology, Dana and David Dornsife College of Letters, Arts and Sciences, University of Southern California, Los Angeles, CA, United States

ARTICLE INFO

Article history:
Received 28 February 2011
Revised 31 August 2011
Accepted 16 September 2011
Available online 24 September 2011

Keywords:
Glucose uptake
p38 MAPK (*M*itogen *A*ctivated *P*rotein *K*inase)
Inflammation
AKT2
Fatty acid oxidation

ABSTRACT

Protease inhibitors (PIs), such as atazanavir sulfate and ritonavir, are used clinically to prevent the progression of HIV and are known to induce insulin resistance. To determine whether PI-mediated insulin resistance is induced by activation of pro-inflammatory cascades, L6 skeletal muscle cells were treated ±atazanavir sulfate, ritonavir, or atazanavir sulfate + ritonavir, and ±insulin. Treatment with atazanavir sulfate, ritonavir, or atazanavir sulfate + ritonavir for 24 or 48 h significantly increased basal glucose uptake ($P < 0.05$) and atazanavir sulfate + ritonavir treatment increased basal glucose uptake significantly more than ritonavir or atazanavir sulfate treatment alone ($P < 0.05$). Atazanavir sulfate + ritonavir treatment for 48 h completely prevented insulin stimulation of glucose uptake ($P > 0.05$). When compared to untreated cells, basal palmitate uptake and oxidation was found to be significantly higher in cells treated with PIs alone or in combination ($P < 0.05$). Prior PI treatment alone or in combination prevented ($P > 0.05$) the insulin-mediated increase in palmitate uptake and the insulin-mediated decrease in palmitate oxidation observed in the control group. Atazanavir sulfate treatment alone or in combination with ritonavir significantly increased JNK1/2 phosphorylation when compared to the control or ritonavir group ($P < 0.05$) and this was accompanied by a rise ($P < 0.05$) in AKT^{Ser473} phosphorylation in the basal state. Total JNK1/2 and p38 MAPK protein content and p38 MAPK phosphorylation state were not altered in any of the treatment groups ($P > 0.05$). Our data indicate that, in muscle cells, PIs induce metabolic dysfunction that is not limited to insulin-sensitive metabolism and that is potentially mediated by a rise in JNK1/2 pro-inflammatory signaling.

1. Introduction

Highly active antiretroviral therapy (HAART), a combination of three types of drugs comprising non-nucleoside reverse transcriptase inhibitors (NNRTIs), nucleoside reverse transcriptase inhibitors (NRTIs) and protease inhibitors (PIs), is used to control replication of the immunodeficiency virus (HIV) and the development of acquired immunodeficiency syndrome (AIDS) in HIV-infected patients (Havlir and Lange, 1998). Treatment of HIV infection with HAART has resulted in declines in morbidity and mortality due to AIDS (Palella et al., 1998). However, despite the clinical successes associated with this drug regimen, it is recognized that many patients treated with HAART develop adverse metabolic consequences which are usually characterized by the presence of peripheral insulin resistance as well as dyslipidemia and fat redistribution (Flint et al., 2009). Given that HIV patients started to demonstrate the clinical symptoms associated with these metabolic pathologies when a cocktail of PIs was introduced in the treatment regimen (Carr et al., 1998; Noor, 2007), the specific role of PIs in the development of HAART-induced metabolic dysfunction remains an important research topic. Most studies investigating the cellular mechanisms responsible for HAART-induced insulin resistance have focused on adipose tissue (Adler-Wailes et al., 2010; Murata et al., 2000; Ranganathan and Kern, 2002) while only limited experimental data are available on the cellular mechanisms by which PI cocktails induce insulin resistance in skeletal muscle.

Insulin resistance in skeletal muscle is a multifactorial pathology which is characterized by reduced insulin action and impairment in fatty acid (FA) and glucose metabolism and whose development has been linked to the presence of inflammation (Bastard et al., 2006; DeFronzo et al., 1992; Shoelson et al., 2006; Shulman, 2000). Given that circulating levels of inflammatory markers such as tumor necrosis factor α receptor (TNFαR) have been shown to be elevated in HIV-infected patients receiving PI-inclusive drug regimens (Mynarcik et al., 2000), inflammation

* Corresponding author at: Department of Kinesiology, Dana and David Dornsife College of Letters, Arts and Sciences, University of Southern California, 3560 Watt Way, PED 107, Los Angeles, CA 90089-0652, United States. Tel.: +1 213 740 8527; fax: +1 213 740 7909.
E-mail address: turcotte@usc.edu (L.P. Turcotte).

0166-3542/$ - see front matter © 2011 Elsevier B.V. All rights reserved.
doi:10.1016/j.antiviral.2011.09.008

may play a significant role in HAART-induced insulin resistance in skeletal muscle cells. Two key intracellular markers of inflammation within skeletal muscle cells include p38 MAPK (*M*itogen *A*ctivated *P*rotein *K*inase) and C-Jun-N-terminal kinase (JNK1/2). These markers have been shown to be upregulated in inflammatory conditions such as obesity and to negatively affect the induction of the insulin signaling cascade (Hirosumi et al., 2002). Thus, if inflammation is a significant mechanism by which PI-induced insulin resistance develops, PIs may upregulate p38 MAPK and JNK1/2.

Given this information, the purpose of this study was to determine in skeletal muscle cells (1) whether short-term chronic exposure to a PI cocktail that includes atazanavir sulfate and ritonavir would negatively impact the regulation of glucose and FA metabolism under basal and insulin-mediated conditions and (2) whether these metabolic alterations would be associated with an upregulation of p38 MAPK and JNK1/2 pro-inflammatory signaling. We hypothesized that PI treatment would increase the activity of pro-inflammatory markers and be associated with muscle insulin resistance as it pertains to both glucose uptake and FA uptake and oxidation. To accomplish our aims, we used the L6 skeletal muscle cell line and treated the cells with atazanavir sulfate and/or ritonavir for up to 48 h. We used atazanavir sulfate and ritonavir because the Department of Health and Human Services Panel on Antiretroviral Guidelines for Adults and Adolescents (2008) recommends their use to maintain an acceptable virologic response while minimizing adverse effects on glucose and lipid metabolism (Panel on Antiretroviral Guidelines for Adults and Adolescents, 2008). To ascertain the independent effects of each PI on cell metabolism and signaling, the responses of cells exposed to both PIs were compared to the responses of cells exposed to one PI only.

2. Materials and methods

2.1. Cell culture

L6 myoblasts were cultured in α-minimal essential medium+ (α-MEM+) containing 10% fetal calf serum (FCS), 1% antibiotic–antimycotic solution (Sigma Aldrich Ltd., St-Louis, MO), and 500 μM L-carnitine (Sigma Aldrich, St. Louis, MO) in a humidified incubator at 37 °C (95% O_2, 5% CO_2). The α-MEM+ and FCS were purchased from the Cell Culture Facility (University of Southern California, Los Angeles, CA). Cells were grown in 75 cm^2 sterile culture flasks, sub-cultured at 60–80% confluence and split at a ratio of 1:10 using trypsin–EDTA (Invitrogen, Grand Island, NY). Cells were sub-cultured into 6-well plates and switched to α-MEM+ containing 2% FCS to promote differentiation. By day 4, cells were 100% confluent and spontaneously differentiated into myotubes. L6 myotubes were 10 days post-confluent on the day of the experiment.

2.2. Cell treatments

Atazanavir sulfate and ritonavir were obtained through the AIDS Research and Reference Reagent Program, Division of AIDS, NIAID, NIH. Cells were first pre-exposed (24, 48, or 72 h) to atazanavir sulfate (100 μM) and/or ritonavir (25 μM) or vehicle (modified α-MEM+, see above) and then incubated with serum-free medium (5 h, for metabolic measurements) and Krebs Ringer Hepes buffer (KRB) (30 min: 1.47 mM K_2HPO_4/140 mM NaCl/1.7 mM KCl/0.9 mM $CaCl_2$/0.9 mM $MgSO_4$/20 mM Hepes; pH 7.4). Cells were then exposed to either insulin (100 nM; Novolin Insulin, University of Southern California Pharmacy) or vehicle (KRB) for 15 min. The cells were then harvested in lysis buffer for Western blot analysis (see below) or subjected to the palmitate uptake and oxidation or glucose uptake assay.

2.3. Palmitate uptake and oxidation

Following each treatment ± insulin, the experimental medium was replaced with transport medium (100 μM albumin-bound palmitate, 1:1, 30 min) containing [1-^{14}C]palmitic acid (4 μCi/mL, Perkin Elmer, Boston, MA) to measure palmitate uptake and oxidation as described previously (Bogachus and Turcotte, 2010; Kelly et al., 2008). Incubations were terminated by removing the media which were used to assay for ^{14}C-labeled oxidation products (see below). Following lysis, one set of duplicate aliquots of the lysate was used to measure protein content using the Bradford method (BioRad, Hercules, CA), while another set was mixed with scintillation fluid (BudgetSolve, Research Product International Corp., Mount Prospect, IL) to count radioactivity (Tri-carb 2100TR analyzer, Packard, Downers Grove, IL). For the measurement of oxidation products, $^{14}CO_2$ was released from duplicate aliquots of experimental media and trapped on filter paper (Whatman). The filter paper was mixed with toluene-based scintillation cocktail and analyzed for $^{14}CO_2$ radioactivity. To correct for carbon loss, additional experiments were conducted with 4 μCi of [1-^{14}C]acetic acid (Perkin Elmer, Boston, MA) instead of [1-^{14}C]palmitic acid (Bogachus and Turcotte, 2010; Kelly et al., 2008).

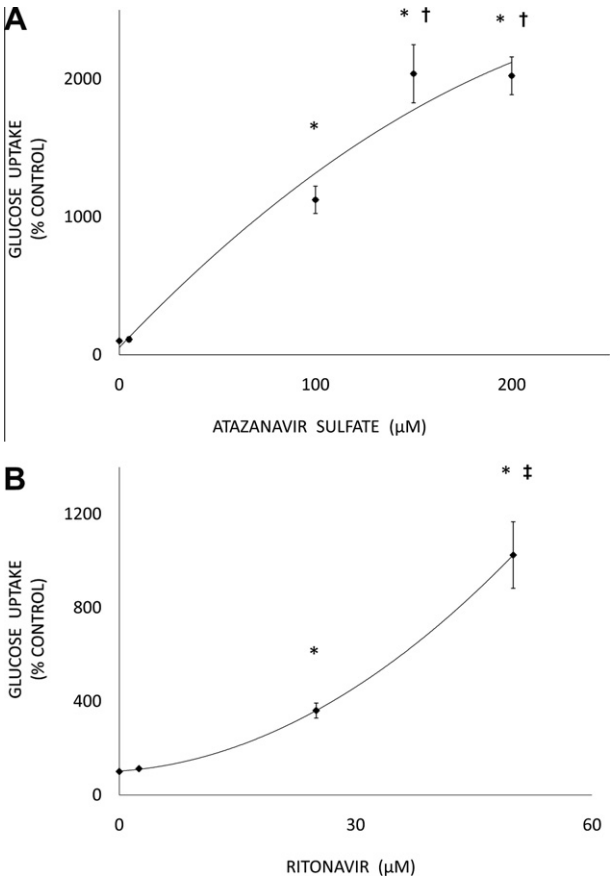

Fig. 1. Dose–response curve for atazanavir sulfate and ritonavir on glucose uptake in L6 cells. Cells were exposed to atazanavir sulfate (0, 5, 100, 150, and 200 μM; A) or ritonavir (0, 2.5, 25, and 50 μM; B) for 48 h. Glucose uptake was measured as described in Methods. Values are mean ± SE for all treatment groups (n = 3–5 per condition) and are expressed as percentage of control, where control refers to cells that are not treated with atazanavir sulfate or ritonavir. $^{*}P < 0.05$ *vs* control and lowest concentration group; $^{\dagger}P < 0.05$ *vs* 100 μM atazanavir sulfate; $^{\ddagger}P < 0.05$ *vs* 25 μM ritonavir.

2.4. Glucose uptake

Following each treatment ± insulin, the experimental medium was replaced with transport medium (200 μM, 5 min) containing [2-^{3}H]deoxyglucose (2-DG) (0.5 μCi/mL, MP Biochemicals, LLC, Solon, OH) to measure glucose uptake (Bogachus and Turcotte, 2010; Kelly et al., 2008). Incubations were terminated via removal of the media and lysis with SDS. As for palmitate uptake, duplicate aliquots of lysate were taken for scintillation counting and for protein determination.

2.5. Western blot analysis

After the experimental treatments, cells were washed with ice cold KRB and prepared for Western blotting as described (Kelly et al., 2010). Lysis buffer was added (20 mM Tris/1% Np-40/137 mM NaCl/1 mM $CaCl_2$/1 mM $MgCl_2$/10% (v/v) glycerol/1 mM DTT/1 mM PMSF/2 mM Na_3VO_4) and cells were gently pelleted via centrifugation. Aliquots of the supernatants were assayed for protein content (Bradford method; Bio-Rad, Hercules, CA) or subjected to 12% SDS polyacrylamide gel electrophoresis. The separated proteins were transferred onto Immobilin-P-polyvinylidene difluoride (PVDF) membranes, blocked, and incubated overnight with primary antibodies (1:1000) to measure either the total protein content for AKT2, or SAPK/JNK, or p38 MAP Kinase (Cell Signaling, Danvers, MA), or the phosphorylation state of AKT^{Ser473}, or SAPH/JNK$^{Thr183/Tyr185}$, or p38 MAP Kinase$^{Thr180/Tyr182}$ (Cell Signaling, Danvers, MA). We chose to measure AKT2 because it is expressed in skeletal muscle of mammalian cells (Bouzakri et al., 2006; Fazakerley et al., 2010), and studies involving AKT2 knockout mice demonstrated the necessity of AKT2 for glucose homeostasis since AKT2 knockout mice could not effectively regulate their glucose levels and developed a type 2 diabetes-like phenotype (Cho et al., 2001; Garofalo et al., 2003; Gonzalez and McGraw, 2009). After exposure to the secondary antibody horseradish peroxidase goat anti-rabbit (1:10,000; Pierce, Rockford, IL), the membranes were developed via enhanced chemiluminescence (Pierce, Rockford, IL) followed by exposure to CL-XPosure film (Pierce, Rockford, IL). Where appropriate, membranes were stripped and re-probed with the GAPDH antibody (Santa Cruz Biotechnologies, Santa Cruz, CA). The films were scanned using a Hewlett Packard ScanJet 6200C and quantified using Scion Image (Scion, Frederick, MD). In all cases, multiple gels were analyzed and compared to results obtained for control cells that had not been treated with atazanavir sulfate, ritonavir, and/or insulin. Protein content was normalized to GAPDH.

2.6. Cell viability

Cell viability was determined via an MTT (3-[4,5-dimethylthiazol-2-yl]-2,5-diphenyl tetrazolium bromide)-based assay (Sigma, St. Louis, MO) that determines mitochondrial function spectrophotometrically (Wang et al., 2010; Xu et al., 2008). Briefly and in line with the Manufacturer's instructions, control cells and cells treated with protease inhibitors were incubated with MTT for 150 min (37 °C). After incubation, the resulting formazan crystals (purple

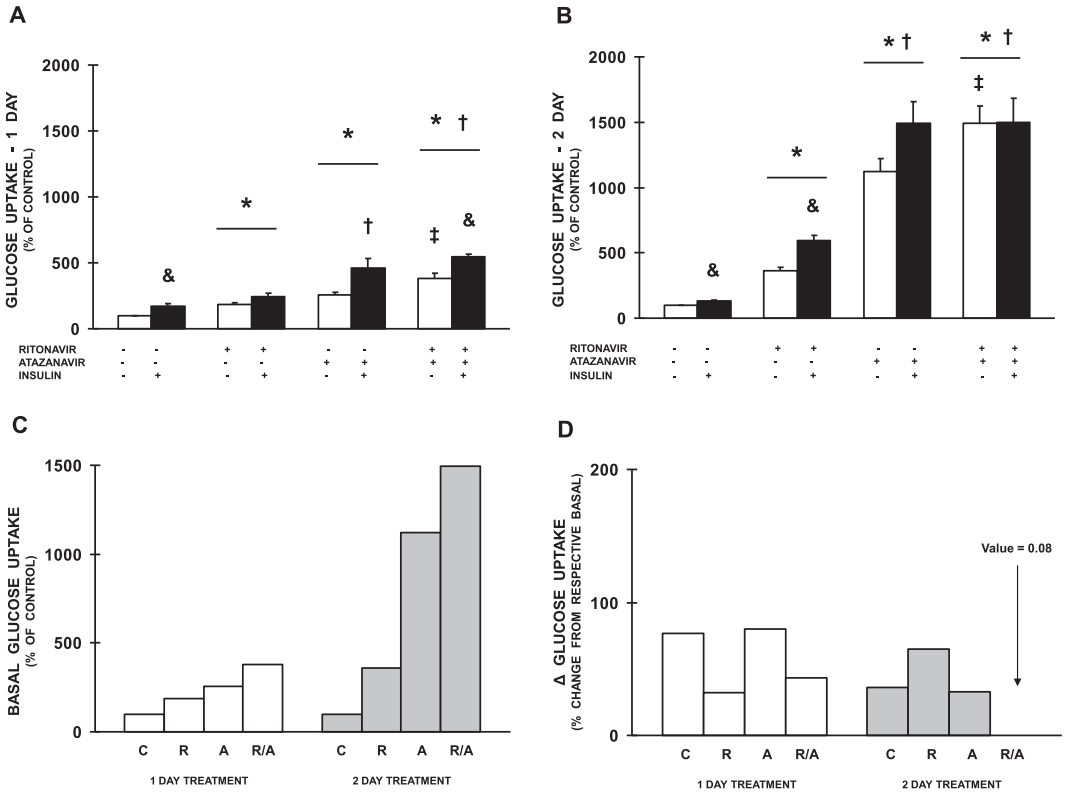

Fig. 2. Effect of atazanavir sulfate and/or ritonavir on the rate of basal and insulin-mediated glucose uptake in L6 cells. Insulin-mediated (100 nM) glucose uptake was assessed after treatment with atazanavir sulfate (100 μM) and/or ritonavir (25 μM) for 24 h (A) or 48 h (B). Values are mean ± SE for all treatment groups (n = 3–6 per condition) and are expressed as percentage of control, where control refers to cells that are not treated with atazanavir sulfate, ritonavir, or insulin. In panel C, basal glucose uptake in each treatment group is expressed as a percent value of basal glucose uptake in the untreated cells. In panel D, Δ glucose uptake represents the percent change in glucose uptake with insulin treatment for each group and was calculated as the average rate of insulin-mediated glucose uptake minus the average rate of basal glucose uptake divided by the average rate of basal glucose uptake. In panels C and D, C refers to the control group (untreated cells), R to the group treated with ritonavir, A to the group treated with atazanavir sulfate and R/A to the group treated with ritonavir and atazanavir sulfate. $^*P < 0.05$ *vs* control treatment; $^{\&}P < 0.05$ *vs* respective treatment in basal state; $^{\dagger}P < 0.05$ *vs* ritonavir treatment; $^{\ddagger}P < 0.05$ *vs* atazanavir sulfate treatment.

color) were solubilized and their absorbance was measured spectrophotometrically at 570 nm, whereas background absorbance was measured at 690 nm. The final absorbance was calculated as absorbance at 570 nm minus the background absorbance measured at 690 nm.

2.7. Calculations and statistics

The rates of glucose and palmitate uptake and of palmitate oxidation were calculated as described in detail (Bogachus and Turcotte, 2010; Kelly et al., 2008). All presented data are expressed as mean ± SE and are expressed as percent of control where control refers to cells that were not treated with any agent or insulin (see Figure legends for specific details). The percent control was calculated using measured rates (nmol/g/min) for all experimental treatments. The effects of the protease inhibitors were analyzed using a one-way ANOVA (Statview) followed by Fisher LSD *post hoc* test when appropriate. The square of the Pearson product moment coefficient was used to determine the significance of correlations when necessary. Insulin-mediated responses were analyzed using *T*-tests when appropriate. In all instances, an α of 0.05 was used to determine significance.

3. Results

3.1. Combined atazanavir sulfate + ritonavir treatment increases basal glucose uptake and induces insulin resistance within 48 h

To ensure that the selected concentrations of atazanavir sulfate and ritonavir were not associated with a maximal glucose uptake response, dose–response curves were completed for both atazanavir sulfate (5, 100, 150, and 200 μM) and ritonavir (2.5, 25, and 50 μM) (Fig 1A and B). Atazanavir sulfate significantly increased glucose uptake in the 100 μM treatment group when compared to the 5 μM treatment and control groups ($P < 0.05$). Glucose uptake in the 150 and 200 μM atazanavir sulfate treatment groups was significantly higher when compared to the control and 5 and 100 μM treatment groups ($P < 0.05$). Similarly, ritonavir significantly increased glucose uptake in the 25 μM treatment group when compared to the 2.5 μM treatment and control groups ($P < 0.05$). Higher levels of ritonavir (50 μM) induced a significantly greater rate of glucose uptake when compared to the ritonavir (2.5 and 25 μM) treatment and control groups ($P < 0.05$). Thus, 100 μM atazanavir sulfate and 25 μM ritonavir were chosen because they were in the middle of the dose–response curve and, as such, did not maximize the glucose uptake system allowing for a further increase in glucose uptake with insulin stimulation.

To determine how time-dependent treatment with atazanavir sulfate and/or ritonavir would affect insulin sensitivity in muscle cells, basal and insulin-mediated glucose uptake were measured in cells incubated with PIs for 24, 48 or 72 h. Because treatment with PIs for 72 h led to significant loss of cell viability (<60% viable), only the 24 and 48-h incubation data are presented. Cell viability at 48-h incubation as assessed by an MTT-based mitochondrial activity assay was greater than 93% ($P < 0.05$). Treatment with atazanavir sulfate, ritonavir, or atazanavir sulfate + ritonavir for 24 or 48 h significantly increased basal glucose uptake ($P < 0.05$) and atazanavir sulfate + ritonavir treatment increased basal glucose uptake significantly more than ritonavir or atazanavir sulfate treatment alone ($P < 0.05$) (Fig 2A–C). Insulin stimulation of glucose uptake was impaired in the 24 and 48-h atazanavir sulfate groups and the 24-h ritonavir group ($P > 0.05$; compared to the basal condition) and was completely prevented

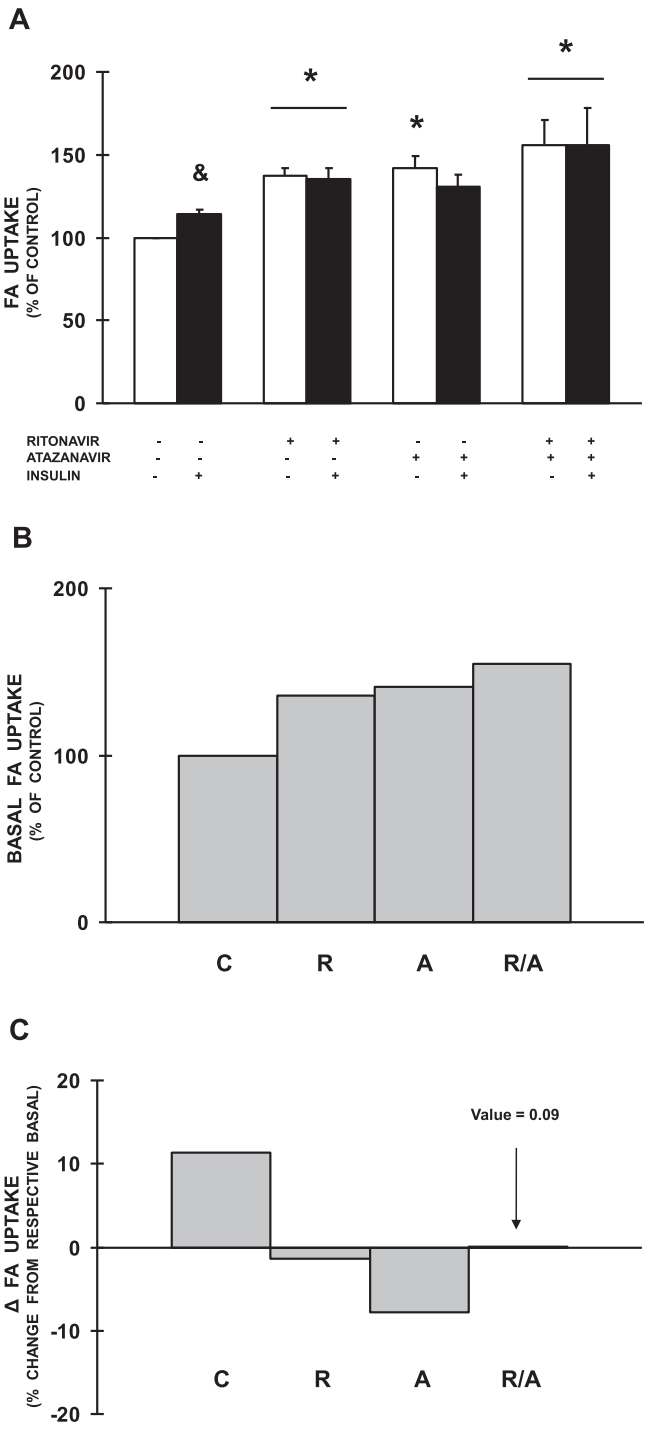

Fig. 3. Effect of atazanavir sulfate and/or ritonavir on the rate of basal and insulin-mediated FA uptake in L6 cells. Insulin-mediated (100 nM) FA uptake was assessed after treatment with atazanavir sulfate (100 μM) and/or ritonavir (25 μM) for 48 h (A). In panel B, basal FA uptake was assessed after treatment with atazanavir sulfate (100 μM) and/or ritonavir (25 μM) for 48 h. Values are mean ± SE for all treatment groups ($n = 3$–4 per condition) and are expressed as percentage of control, where control refers to cells that are not treated with atazanavir sulfate, ritonavir, or insulin. In panel C, Δ FA uptake represents the percent change in FA uptake with insulin treatment for each group and was calculated as the average rate of insulin-mediated FA uptake minus the average rate of basal FA uptake divided by the average rate of basal FA uptake. In panels B and C, C refers to the control group (untreated cells), R to the group treated with ritonavir, A to the group treated with atazanavir sulfate and R/A to the group treated with ritonavir and atazanavir sulfate. $^{*}P < 0.05$ *vs* control treatment; $^{\&}P < 0.05$ *vs* respective treatment in basal state.

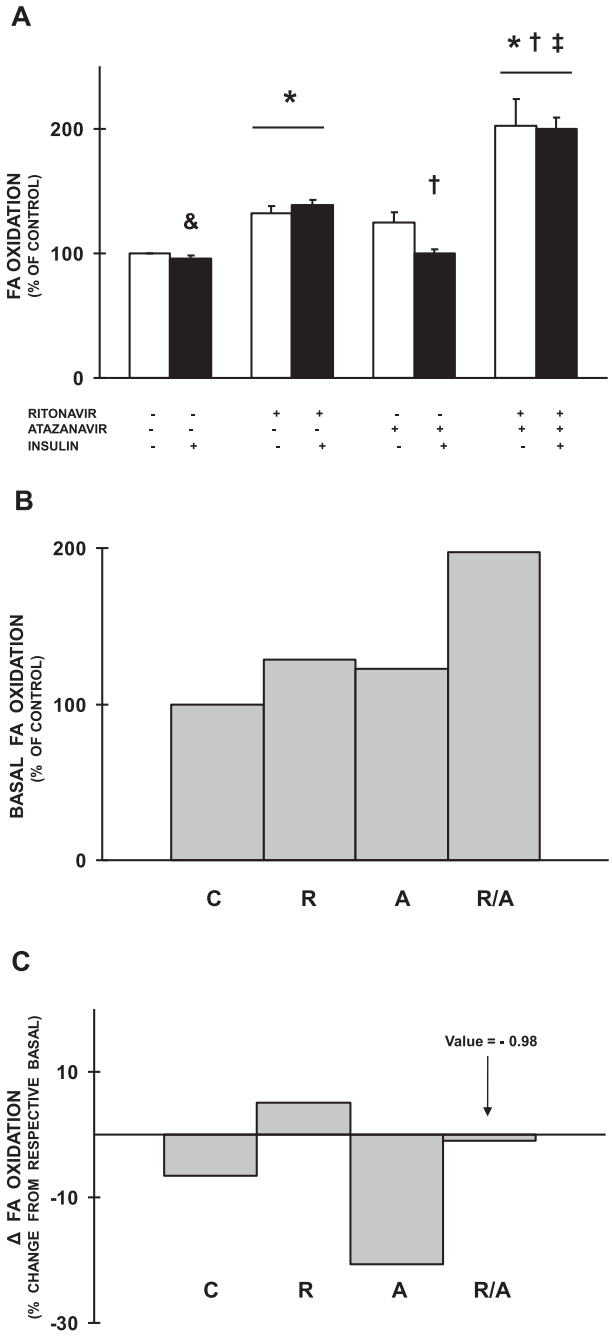

Fig. 4. Effect of atazanavir sulfate and/or ritonavir on the rate of basal and insulin-mediated FA oxidation in L6 cells. Insulin-mediated (100 nM) FA oxidation was assessed after treatment with atazanavir sulfate (100 μM) and/or ritonavir (25 μM) for 48 h (A). In panel B, basal FA uptake was assessed after treatment with atazanavir sulfate (100 μM) and/or ritonavir (25 μM) for 48 h. Values are mean ± SE for all treatment groups (n = 3–4 per condition) and are expressed as percentage of control, where control refers to cells that are not treated with atazanavir sulfate, ritonavir, or insulin. In panel C, Δ FA oxidation represents the percent change in FA oxidation with insulin treatment for each group and was calculated as the average rate of insulin-mediated FA oxidation minus the average rate of basal FA oxidation divided by the average rate of basal FA oxidation. In panels B and C, C refers to the control group (untreated cells), R to the group treated with ritonavir, A to the group treated with atazanavir sulfate and R/A to the group treated with ritonavir and atazanavir sulfate. $^{*}P < 0.05$ *vs* control treatment; $^{\&}P < 0.05$ *vs* respective treatment in basal state; $^{\dagger}P < 0.05$ *vs* ritonavir treatment; $^{\ddagger}P < 0.05$ *vs* atazanavir sulfate treatment.

in the 48-h atazanavir sulfate + ritonavir group ($P > 0.05$; compared to the basal condition) (Fig 2A, B, and D).

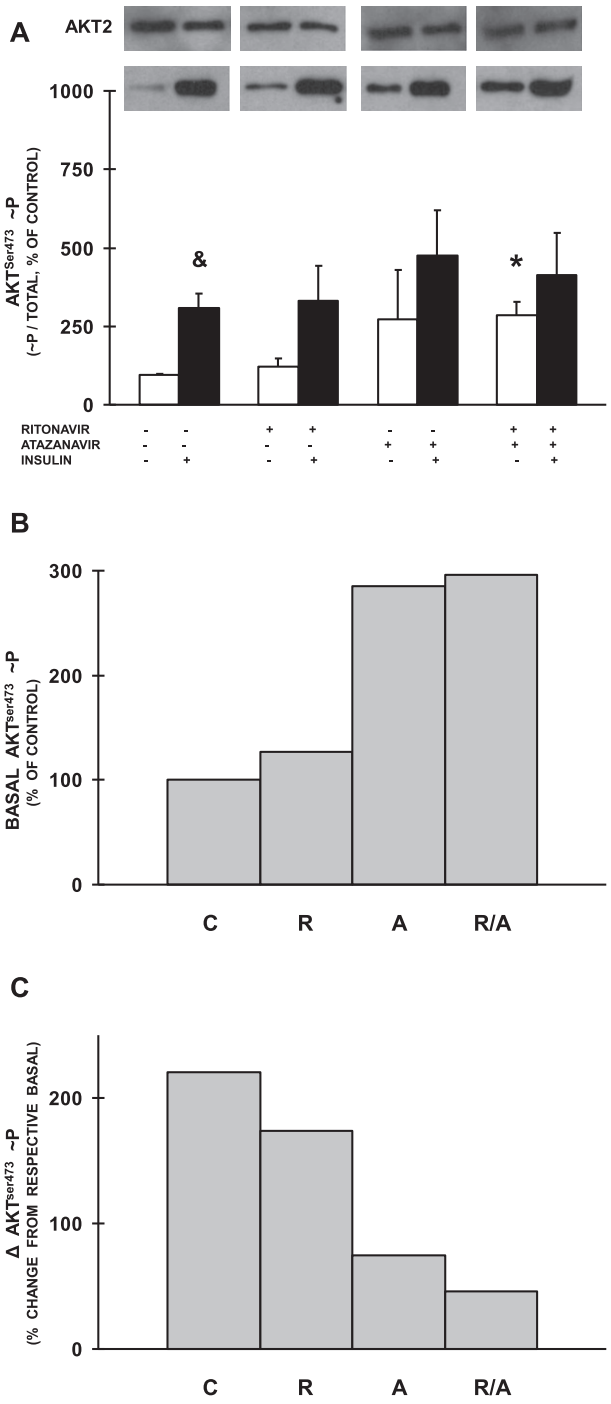

Fig. 5. Effect of atazanavir sulfate and/or ritonavir on basal and insulin-mediated AKT^{Ser473} phosphorylation in L6 cells. Insulin-mediated (100 nM) AKT^{Ser473} phosphorylation was assessed after treatment with atazanavir sulfate (100 μM) and/or ritonavir (25 μM) for 48 h (A). Top panel of representative gels in (A) illustrate total AKT2 protein content, while bottom panel represents AKT^{Ser473} phosphorylation. In panel B, basal AKT^{Ser473} phosphorylation was assessed after treatment with atazanavir sulfate (100 μM) and/or ritonavir (25 μM) for 48 h. Values are mean ± SE for all treatment groups (n = 3–6 per condition) and are expressed as percentage of control, where control refers to cells that are not treated with atazanavir sulfate, ritonavir, or insulin. In panel C, Δ AKT^{Ser473} phosphorylation represents the percent change in AKT^{Ser473} phosphorylation with insulin treatment for each group and was calculated as the average rate of insulin-mediated AKT^{Ser473} phosphorylation minus the average rate of basal AKT^{Ser473} phosphorylation divided by the average rate of basal AKT^{Ser473} phosphorylation. In panels B and C, C refers to the control group (untreated cells), R to the group treated with ritonavir, A to the group treated with atazanavir sulfate and R/A to the group treated with ritonavir and atazanavir sulfate. $^{*}P < 0.05$ *vs* control treatment; $^{\&}P < 0.05$ *vs* respective treatment in basal state.

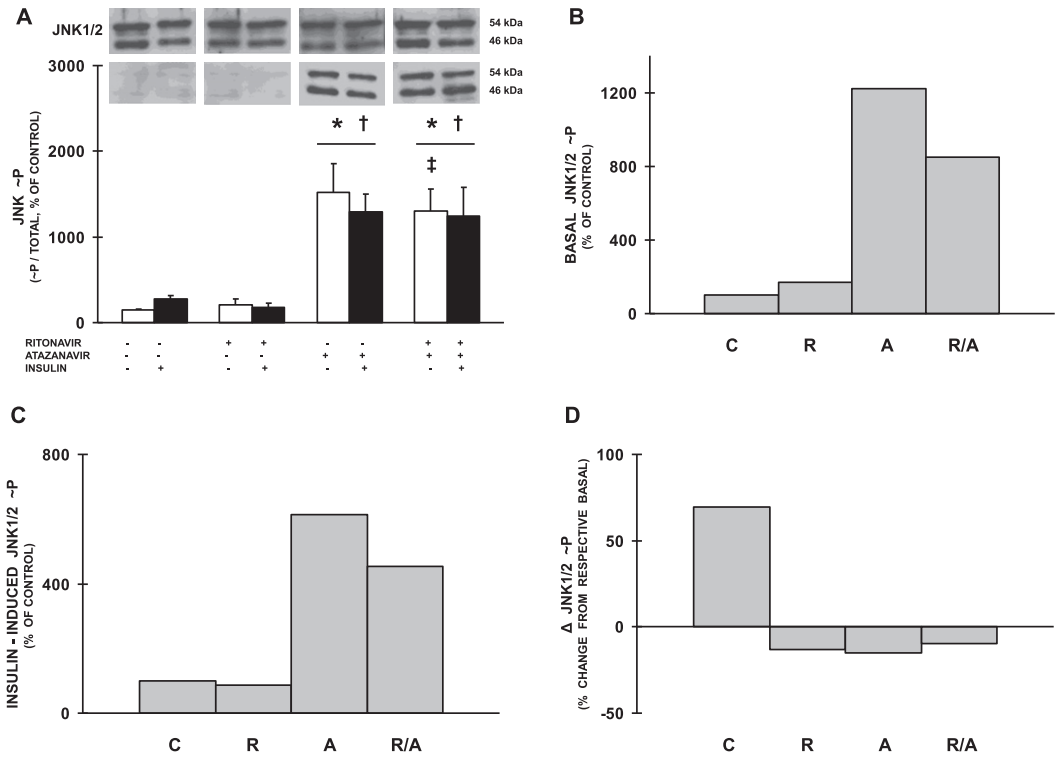

Fig. 6. Effect of atazanavir sulfate and/or ritonavir on basal and insulin-mediated JNK1/2 phosphorylation in L6 cells. Insulin-mediated (100 nM) JNK1/2 phosphorylation was assessed after treatment with atazanavir sulfate (100 μM) and/or ritonavir (25 μM) for 48 h (A). Top panel of representative gels in (A) illustrate total JNK1/2 protein content, while bottom panel represents JNK1/2 phosphorylation. In panel B, basal JNK1/2 phosphorylation was assessed after treatment with atazanavir sulfate (100 μM) and/or ritonavir (25 μM) for 48 h. Values are expressed as percentage of control, where control refers to cells that are not treated with atazanavir sulfate, ritonavir, or insulin. In panel C, insulin-induced JNK1/2 phosphorylation was assessed after treatment with atazanavir sulfate (100 μM) and/or ritonavir (25 μM) for 48 h +insulin (100 nM, 15 min). Values are expressed as percentage of control, where control refers to cells that are not treated with atazanavir sulfate or ritonavir. Values are mean ± SE for all treatment groups (n = 3–8 per condition). In panel D, Δ JNK1/2 phosphorylation represents the percent change in JNK1/2 phosphorylation with insulin treatment for each group and was calculated as the average rate of insulin-mediated JNK1/2 phosphorylation minus the average rate of basal JNK1/2 phosphorylation divided by the average rate of basal JNK1/2 phosphorylation. In panels B, C, and D, C refers to the control group (untreated cells), R to the group treated with ritonavir, A to the group treated with atazanavir sulfate and R/A to the group treated with ritonavir and atazanavir sulfate. *$P < 0.05$ *vs* control treatment; †$P < 0.05$ *vs* ritonavir treatment; ‡$P < 0.05$ *vs* atazanavir sulfate treatment.

3.2. Combined atazanavir sulfate + ritonavir treatment increases basal palmitate uptake and oxidation and prevents insulin-mediated changes

To determine how the induction of insulin resistance *via* atazanavir sulfate + ritonavir treatment would affect FA metabolism, basal and insulin-mediated palmitate uptake and oxidation were measured in cells treated with PIs for 48 h. Basal palmitate uptake (35–41%) and oxidation (22–28%) was found to be significantly ($P < 0.05$) higher in cells treated with PIs alone or in combination when compared to untreated cells ($P < 0.05$) (Fig. 3A and B, 4A and B). The increase in basal palmitate oxidation (97%) was found to be significantly higher ($P < 0.05$) when the cells were treated with both ritonavir and atazanavir sulfate. Prior treatment with atazanavir sulfate or ritonavir alone or in combination prevented ($P > 0.05$ *vs* the basal condition) the insulin-mediated increase in palmitate uptake (Fig 3A and C) and the insulin-mediated decrease in palmitate oxidation (Fig 4A and C) observed in untreated cells.

3.3. Combined atazanavir sulfate + ritonavir treatment prevents insulin-mediated AKT^{Ser473} phosphorylation

To assess the impact of atazanavir sulfate and/or ritonavir treatment on insulin signaling, AKT2 protein content and phosphorylation state were measured. Total AKT2 protein content was not affected by any of the treatments ($P > 0.05$) (Fig 5A). In line with the glucose uptake data, basal AKT^{Ser473} phosphorylation was higher (196%) in the atazanavir sulfate + ritonavir group when compared to the control group ($P < 0.05$) (Fig 5A and B) and the insulin-induced increase in AKT^{Ser473} phosphorylation observed in the control group (220%) was prevented by treatment with atazanavir sulfate, ritonavir, or atazanavir sulfate + ritonavir ($P > 0.05$) (Fig 5A and C). AKT^{Ser473} phosphorylation was positively correlated ($R^2 = 0.94$; $P < 0.05$) with glucose uptake under basal conditions but not FA oxidation ($R^2 = 0.08$; $P > 0.05$) (data not shown).

3.4. Atazanavir sulfate treatment alone or in combination with ritonavir increases JNK1/2 phosphorylation but does not alter p38 MAPK phosphorylation

Inflammation has been shown to play a significant role in the induction of insulin resistance in muscle cells (Dandona et al., 2004). Therefore, two markers of inflammation, JNK1/2 and p38 MAPK, were measured to assess the role of inflammation in PI-induced insulin resistance in muscle cells. Total JNK1/2 protein content in the basal state was not affected by PI treatment ($P > 0.05$) (Fig 6A). However, total JNK1/2 protein content in the insulin-mediated state was found to be higher in the atazanavir sulfate + ritonavir group when compared to the atazanavir sulfate group or ritonavir group ($P < 0.05$) but not when compared to the control group ($P > 0.05$). Atazanavir sulfate treatment alone or in combination with ritonavir significantly increased basal (7- to 11-fold) and insulin-mediated (3- to 5-fold) JNK1/2 phosphorylation when compared to the control or ritonavir group ($P < 0.05$) (Fig 6B and C). JNK1/2 phosphorylation was positively correlated ($R^2 = 0.74$; $P < 0.05$) with glucose uptake but not FA oxidation ($R^2 = 0.08$;

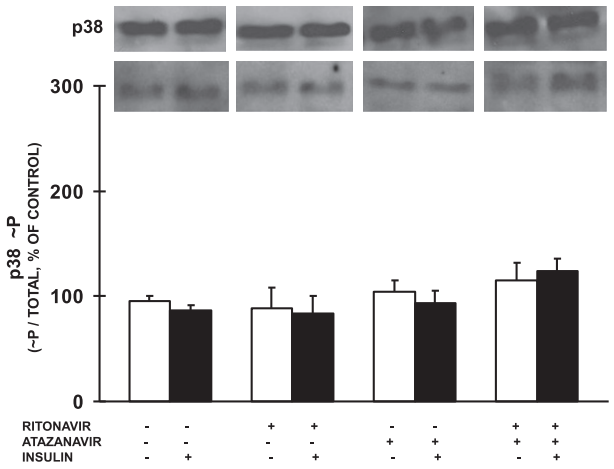

Fig. 7. Effect of atazanavir sulfate and/or ritonavir on basal and insulin-mediated p38 MAPK phosphorylation in L6 cells. Insulin-mediated (100 nM) p38 MAPK phosphorylation was assessed after treatment with atazanavir sulfate (100 μM) and/or ritonavir (25 μM) for 48 h. Top panel of representative gels illustrate total p38 protein content, while bottom panel represents p38 phosphorylation. Values are mean ± SE for all treatment groups (n = 3–5 per condition) and are expressed as percentage of control, where control refers to cells that were not treated with atazanavir sulfate, ritonavir, or insulin.

$P > 0.05$) (data not shown). Total p38 MAPK protein content and p38 MAPK phosphorylation state were not altered in any of the treatment groups ($P > 0.05$) (Fig 7).

4. Discussion

Our data provide new mechanistic insights for PI-induced metabolic dysfunction in skeletal muscle cells and implicate the JNK1/2 pro-inflammatory signaling cascade in the loss of insulin sensitivity with PI treatment. Most importantly, our results show that PI treatment significantly impacts both basal and insulin-mediated muscle metabolism. Thus, basal rates of glucose uptake and FA uptake and oxidation were increased by short-term chronic PI treatment and these metabolic alterations were associated with increased JNK1/2 phosphorylation and AKT^{Ser473} phosphorylation. Our data also show that short-term chronic PI treatment completely prevented an increase in insulin-induced AKT^{Ser473} phosphorylation and negatively affected insulin-mediated metabolic regulation of glucose uptake, FA uptake and FA oxidation suggesting that PI-induced activation of the JNK1/2 pro-inflammatory cascade is a primary event that significantly impacts proximal insulin signaling and insulin-mediated metabolic regulation.

Very little research has been done looking at the effects of PI treatment on FA uptake and/or oxidation in skeletal muscle cells. Herein, we show that metabolic impairment associated with short-term chronic PI treatment is not limited to insulin-mediated glucose uptake but that in fact it includes significant changes in basal FA uptake and oxidation as well as a loss in insulin-mediated changes in FA uptake and oxidation. Most significant was the 97% increase in basal FA oxidation, without a similar increase in FA uptake, when cells were treated with both ritonavir and atazanavir sulfate. In line with other data collected in C3H10T1/2 mesenchymal stem cells (Lenhard et al., 2000) and 3T3-L1 adipocytes (Adler-Wailes et al., 2010; Ranganathan and Kern, 2002) in which triglyceride lipolysis was found to be higher with PI treatment, our data suggest that PI treatment stimulates lipid catabolism under non-insulin stimulated conditions. On the other hand, given that HIV-infected patients on HAART therapy have been shown to have higher intramyocellular lipid (IMCL) content in leg muscles when compared to non-HIV-infected control subjects (Gan et al., 2002; Torriani et al., 2006), our results suggest that higher basal rates of FA oxidation may not be the primary mechanism by which IMCL accumulates in HIV-infected patients. In contrast to our results, data from a recent study (Richmond et al., 2010) showed that atazanavir sulfate and ritonavir in combination decreased FA oxidation under basal conditions. This difference in results may have been due in large part to the fact that in the aforementioned study C2C12 muscle cells were pre-exposed to high FA levels for at least 18 h before FA oxidation measurements were assessed. Given that exposure to high FA levels is known to significantly impact basal FA oxidation (Constantinescu and Turcotte, 2010; Pimenta et al., 2008), these differences in results are not unexpected. In fact, we have also shown that high FA exposure (12 h) decreases basal FA oxidation in L6 muscle cells (Constantinescu and Turcotte, 2010).

In line with the presence of insulin resistance, our data show that PI treatment alone or in combination prevented the insulin-mediated increase of FA uptake and suppression of FA oxidation normally observed in healthy untreated muscle (Bogachus and Turcotte, 2010; Dyck et al., 2001; Kelly et al., 2008). Our data agree with results showing reduced insulin-mediated suppression of whole-body fat oxidation during hyperinsulinemia in HIV-infected patients undergoing PI therapy when compared to HIV-infected individuals naïve to PI treatment (Gan et al., 2002).

It is well accepted that cellular inflammation is associated with metabolic dysregulation (Bastard et al., 2006; Shoelson et al., 2006) and may be a causative factor in the development of insulin resistance (Dandona et al., 2004). In line with this notion, our data indicate that activation of the JNK1/2 pro-inflammatory cascade may play a significant role not only in PI-induced insulin resistance but also in the development of metabolic impairment under non-insulin-mediated conditions. Although increased gene and protein expression of pro-inflammatory cytokines has been measured in HIV-infected patients on HAART (Lihn et al., 2003; Sevastianova et al., 2008), conclusions on the independent effects of PI treatment on inflammation are difficult to draw because the HIV virus as well as the NRTIs and/or NNRTIs included in HAART may also have independent effects on inflammation. Here, we show that atazanavir sulfate treatment is associated with a significant activation of the JNK1/2 pro-inflammatory cascade suggesting that, as shown in dietary and genetic models of insulin resistance (Hirosumi et al., 2002) sustained JNK1/2 activation contributes significantly to metabolic dysfunction. Interestingly, PI-mediated JNK1/2 activation was associated with an increase in AKT^{Ser473} phosphorylation. Our data are in line with results showing concurrent stimulation of inflammatory or stress signaling and AKT^{Ser473} phosphorylation in rat hippocampus after forebrain ischemia (Zhang et al., 2007), in 3T3-L1 adipocytes following short-term palmitate treatment (McCall et al., 2010) and in muscle in high fat fed mice (Liu et al., 2009). In agreement with the notion that induction of the JNK1/2 pro-inflammatory cascade is linked to metabolic dysfunction (Hirosumi et al., 2002; Solinas et al., 2006), short-term chronic PI treatment was also associated with an inability to further increase AKT^{Ser473} phosphorylation with insulin stimulation. A similar suppression of insulin-induced AKT^{Ser473} phosphorylation has also been observed in L6 cells following short-term but not acute PI treatment (Ben-Romano et al., 2003; Nolte et al., 2001) and in muscle of HIV-infected patients on HAART (Haugaard et al., 2005). Together with data showing that signaling intermediates upstream and downstream of AKT are also negatively affected by PI treatment (Ben-Romano et al., 2004; Djedaini et al., 2009; Kachko et al., 2009) and that phosphatidylinositol 3-kinase-dependent insulin signaling is critical for the regulation of insulin-mediated FA and glucose metabolism in muscle cells (Bandyopadhyay et al., 1997; Kelly et al., 2008), our data suggest that short-term chronic PI treatment significantly impairs proximal insulin signaling and is a causal factor in the inability of PI-treated muscle cells to respond normally to insulin.

As observed for FA uptake and oxidation, glucose uptake under non-insulin-stimulated conditions was increased by short-term chronic PI treatment. To the best of our knowledge, only one study has reported basal glucose uptake data in L6 cells treated with a specific PI for a similar duration (18 h) (Ben-Romano et al., 2003) and our results agree with those previously reported data. Furthermore, a similar activation of glucose uptake was recorded in L6 cells treated with selective PIs for 8 days (Germinario et al., 2003) and in 3T3-L1 adipocytes treated with selective PIs for a similar duration (18 h to 8 days) (Ben-Romano et al., 2003; Ranganathan and Kern, 2002; Rudich et al., 2001). Our data demonstrating a significant or total suppression of insulin-mediated stimulation of glucose uptake with short-term chronic PI treatment were expected. Indeed, acute PI exposure has been shown to decrease insulin-stimulated glucose uptake in muscle incubated with physiological levels of insulin and whole-body glucose disposal measured in vivo during euglycemic–hyperinsulinemic clamp conditions (Ben-Romano et al., 2003; Hruz et al., 2002; Nolte et al., 2001).

To the best of our knowledge we are the first group to investigate inflammation as a causative factor in the development of metabolic dysfunction and insulin resistance in skeletal muscle cells following short-term chronic treatment with atazanavir sulfate and ritonavir. More specifically, our data show that PI treatment induces significant metabolic alterations in glucose uptake, FA uptake and FA oxidation under basal conditions and that these changes are correlated with a rise in JNK1/2 pro-inflammatory signaling (Fig 8). To determine the link between upregulation of pro-inflammatory signaling and insulin resistance with PI treatment, future studies should focus on investigating the effects of pharmacological or genetic inhibition of pro-inflammatory pathways on the development of insulin resistance. Additionally, since metabolic alterations were observed, the expression of proteins that regulate metabolic processes such as Glut4, CD36, and Acetyl CoA Carboxylase (ACC) should be investigated as potential intracellular mechanisms by which glucose uptake, FA uptake and FA oxidation are increased with atazanavir sulfate and/or ritonavir treatment. Ultimately, studies testing the applicability of the proposed mechanism will need to include whole body animal studies and HIV-infected patients. Clinically, an understanding of the mechanism by which PIs induce insulin resistance would benefit HIV-infected patients because they may lead to the development of alternative drug regimens.

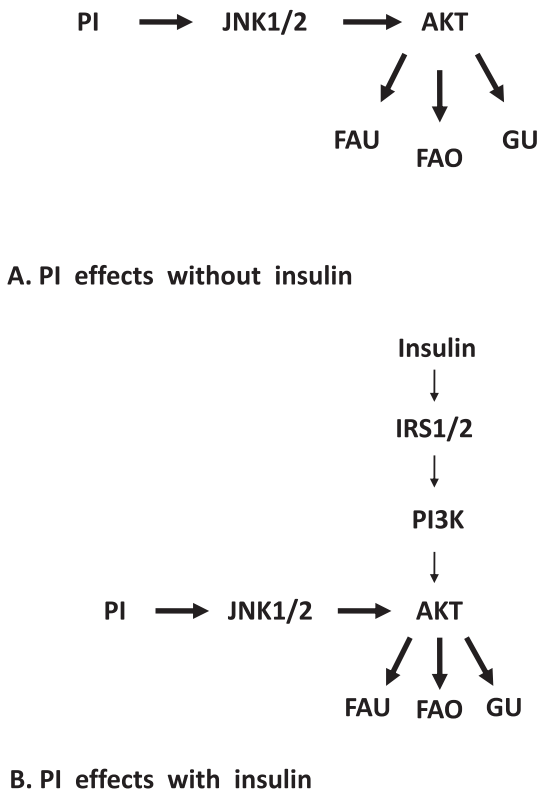

Fig. 8. Schematic representation of proposed cellular mechanisms induced by atazanavir sulfate/ritonavir treatment in L6 cells. As shown in panel A, our data show that short-term (48 h) PI treatment with atazanavir sulfate/ritonavir at the concentrations used in this study induces a pro-inflammatory state which is characterized in part by an activation of JNK1/2 and AKT. Panel B shows that the PI-induced pro-inflammatory state prevents further AKT activation with insulin resulting in resistance to the actions of insulin in metabolic regulation (as evidenced by a loss of insulin-mediated increase in glucose uptake). PI: protease inhibitor.

Acknowledgements

The authors thank Benjamin Shin for his valuable technical assistance. This study was supported, in part, by a grant from the University of Southern California Women in Science and Engineering (WiSE) program, a research grant from the American College of Sports Medicine, and by Fellowships from the Integrative and Evolutionary Biology Program.

References

Adler-Wailes, D.C., Guiney, E.L., Wollins, N.E., Yanovski, J.A., 2010. Long-term ritonavir exposure increases fatty acid and glycerol recycling in 3T3-L1 adipocytes as compensatory mechanisms for increased triacyglcerol hydrolysis. Endocrinology 151, 2097–2105.

Bandyopadhyay, G., Standaert, M.L., Galloway, L., Moscat, J., Farese, R.V., 1997. Evidence for involvement of protein kinase C (PKC)-z and noninvolvement of diacylglycerol-sensitive PKCs in insulin-stimulated glucose transport in L6 myotubes. Endocrinology 138, 4721–4731.

Bastard, J., Maachi, M., Lagathu, C., Kim, M., Caron, M., Vidal, H., Capeau, J., Feve, B., 2006. Recent advances in the relationship between obesity, inflammation, and insulin resistance. European Cytokine Network 17, 4–12.

Ben-Romano, R., Rudich, A., Tirosh, A., Potashnik, R., Sasaoka, T., Riesenberg, K., Schlaeffer, F., Bashan, N., 2004. Nelfinavir-induced insulin resistance is associated with impaired plasma membrane recruitment of the PI 3-kinase effectors Akt/PKB and PKC-z. Diabetologia 47, 1107–1117.

Ben-Romano, R., Rudich, A., Torok, D., Vanounou, S., Riesenberg, K., Schlaeffer, F., Klip, A., Bashan, N., 2003. Agent and cell-type specificity in the induction of insulin resistance by HIV protease inhibitors. AIDS 17, 23–32.

Bogachus, L.D., Turcotte, L.P., 2010. Genetic downregulation of AMPKa isoforms uncovers the mechanism by which metformin decreases FA uptake and oxidation in skeletal muscle cells. American Journal of Physiology. Cell Physiology 299, C1549–C1561.

Bouzakri, K., Zachrisson, A., Al-Khalili, L., Zhang, B.B., Koistinen, H.A., Krook, A., Zierath, J.R., 2006. SiRNA-based gene silencing reveals specialized roles of IRS-1/Akt2 and IRS-2/Akt1 in glucose and lipid metabolism in human skeletal muscle. Cell Metabolism 4, 89–96.

Carr, A., Samaras, K., Burton, S., Law, M., Freund, J., Chisholm, D.J., Cooper, D.A., 1998. A syndrome pf peripheral lipodystrophy, hyperlipidaemia and insulin resistance in patients receiving HIV protease inhibitors. AIDS 12, F51–F58.

Cho, H., Mu, J., Kim, J.K., Thorvaldsen, J.L., Chu, Q., Crenshaw, E.B.I., Kaestner, K.H., Bartolomei, M.S., Shulman, G.I., Birnbaum, M.J., 2001. Insulin resistance and a diabetes mellitus-like syndrome in mice lacking the protein kinase Akt2 (PKBb). Science 292, 1728–1731.

Constantinescu, S., Turcotte, L.P., 2010. Low RIP140 expression partially restores metabolic flexibility in L6 muscle cells treated with high FA. FASEB Journal 24, 1045.3.

Dandona, P., Aljada, A., Bandyopadhyay, A., 2004. Inflammation: the link between insulin resistance, obesity, and diabetes. TRENDS in Immunology 25, 4–7.

DeFronzo, R.A., Bonadonna, R.C., Ferrannini, E., 1992. Pathogenesis of NIDDM. A balanced overview. Diabetes Care 15, 318–368.

Djedaini, M., Peraldi, P., Drici, M.-D., Darini, C., Saint-Marc, P., Dani, C., Ladoux, A., 2009. Lopinavir co-induces insulin resistance and ER stress in human adipocytes. Biochemical and Biophysical Research Communications 386, 96–100.

Dyck, D.J., Steinberg, G., Bonen, A., 2001. Insulin increases FA uptake and esterification but reduces lipid utilization in isolated contracting muscle. American Journal of Physiology. Endocrinology and Metabolism 281, E600–E607.

Fazakerley, D., Holman, G., Marley, A., James, D., Stockli, J., Coster, A., 2010. Kinetic evidence for unique regulation of GLUT4 trafficking by insulin and AMP-

activated protein kinase activators in L6 myotubes. Journal of Biological Chemistry 285, 1653–1660.
Flint, O.P., Noor, M.A., Hruz, P.W., Hylemon, P.B., Yarasheski, K.E., Kotler, D.P., Parker, R.A., Bellamine, A., 2009. The role of protease inhibitors in the pathogenesis of HIV-associated lipodystrophy: cellular mechanisms and clinical implications. Toxicology Pathology 37, 65–77.
Gan, S.K., Samaras, K., Thompson, C.H., Kraegen, E.W., Carr, A., Cooper, D.A., Chisholm, D.J., 2002. Altered myocellular and abdominal fat partitioning predict disturbance in insulin action in hiv protease inhibitor-related lipodystrophy. Diabetes 51, 3163–3169.
Garofalo, R.S., Orena, S.J., Rafidi, K., Torchia, A.J., Stock, J.L., Hildebrandt, A.L., Coskran, T., Black, S.C., Brees, D.J., Wicks, J.R., McNeish, J.D., Coleman, K.G., 2003. Severe diabetes, age-dependent loss of adipose tissue, and mild growth deficiency in mice lacking Akt2/PKBb. Journal of Clinical Investigation 112, 197–208.
Germinario, R., Colby-Germinario, S.P., Cammalleri, C., Wainberg, M., 2003. The long-term effects of anti-retroviral protease inhibitors on sugar transport in L6 cells. Journal of Endocrinology 178, 449–456.
Gonzalez, E., McGraw, T.E., 2009. The AKT kinases: isoform specificity in metabolism and cancer. Cell Cycle 8, 2502–2508.
Haugaard, S.B., Anderson, O., Madsbad, S., Frosig, C., Iversen, J., Nielsen, J., Wojtaszewski, J., 2005. Skeletal muscle insulin signaling defects downstream of phosphatidylinositol 3-kinase at the level of AKT are associated with impaired nonoxidative glucose disposal in HIV lipodystrophy. Diabetes 54, 3474–3483.
Havlir, D., Lange, J., 1998. New antiretrovirals and new combinations. AIDS 12, S165–S174.
Hirosumi, J., Tuncman, G., Chang, L., Gorgun, C.Z., Uysal, K.T., Maeda, K., Karin, M., Hotamisligil, G.S., 2002. A central role for JNK in obesity and insulin resistance. Nature 420, 333–336.
Hruz, P.W., Murata, H., Qiu, H., Mueckler, M., 2002. Indinavir induces acute and reversible peripheral insulin resistance in rats. Diabetes 51, 937–942.
Kachko, I., Maissel, A., Mazor, L., Ben-Romano, R., Watson, R.T., Hou, J.C., Pessin, J.E., Bashan, N., Rudich, A., 2009. Postreceptor adipocyte insulin resistance induced by Nelfinavir is caused by insensitivity of pkb/akt to phosphatidylinositol-3,4,5-triphosphate. Endocrinology 150, 2618–2626.
Kelly, K.R., Abbott, M.J., Turcotte, L.P., 2010. Short-term AMP-regulated protein kinase activation enhances insulin-sensitive fatty acid uptake and increases the effects of insulin on fatty acid oxidation in L6 muscle cells. Experimental Biology and Medicine 235, 514–521.
Kelly, K.R., Sung, C.K., Abbott, M.J., Turcotte, L.P., 2008. Phosphatidylinositol 3-kinase-dependent insulin regulation of long-chain fatty acid (LCFA) metabolism in L6 cells: involvement of atypical protein kinase C-z in LCFA uptake but not oxidation. Journal of Endocrinology 198, 375–384.
Lenhard, J.M., Furfine, E.S., Jain, R.G., Ittoop, O., Orband-Miller, L.A., Blanchrad, S.G., Paulik, M.A., Weiel, J.E., 2000. HIV protease inhibitors block adipogenesis and increase lipolysis in vitro. Antiviral Research 47, 121–129.
Lihn, A.S., Richelsen, B., Pedersen, S.B., Haugaard, S.B., Soby Rathje, G., Madsbad, S., Andersen, O., 2003. Increased expression of TNFa, IL-6, and IL-8 in HALS: implications for reduced adiponectin expression and plasma levels. American Journal of Physiology. Endocrinology and Metabolism 285, E1072–E1080.
Liu, H.-Y., Hong, T., Wen, G.-B., Han, J., Zuo, D., Liu, Z., Cao, W., 2009. Increased basal level of Akt-dependent insulin signaling may be responsible for the development of insulin resistance. Am J. Physiol. Endocrinol. Metab. 297, E898–E906.
McCall, K.D., Holliday, D., Dickerson, E., Wallace, B., Schwartz, A.L., Schwartz, C., Lewis, C.J., Kohn, L., Schwartz, F.L., 2010. Phenylmethimazole blocks palmitate-mediated induction of inflammatory cytokine pathways in 3T3-L1 adipocytes and RAW 264.7 macrophages. Journal of Endocrinology 207, 343–353.
Murata, H., Hruz, P.W., Mueckler, M., 2000. The mechanism of insulin resistance caused by HIV protease inhibitor therapy. Journal of Biological Chemistry 27, 20251–20254.
Mynarcik, D.C., McNurlan, M.A., Steigbigel, R.T., Fuhrer, J., Gelato, M.C., 2000. Association of severe insulin resistance with both loss of limb fat and elevated serum tumor necrosis factor receptor levels in HIV lipodystrophy. JAIDS 25, 312–321.
Nolte, L.A., Yarasheski, K.E., Kawanaka, K., Fisher, J., Le, N., Holloszy, J.O., 2001. The HIV protease inhibitor indinavir decreases insulin- and contraction-stimulated glucose transport in skeletal muscle. Diabetes 50, 1397–1401.
Noor, M.A., 2007. The role of protease inhibitors in the pathogenesis of HIV-associated insulin resistance: cellular mechanisms and clinical implications. Current HIV/AIDS Reports 4, 126–134.
Palella, F.J., Delaney, K.M., Moorman, A.C., Loveless, M.O., Fuhrer, J., Satten, G.A., Aschman, D.J., Holmberg, S.D., 1998. Declining morbidity and mortality among patients with advanced human immunodeficiency virus infection. New England Journal of Medicine 338, 853–860.
Pimenta, A.S., Gaidhu, M.P., Habib, S., So, M., Fediuc, S., Mirpourian, M., Musheev, M., Curi, R., Ceddia, R.B., 2008. Prolonged exposure to palmitate impairs fatty acid oxidation despite activation of AMP-activated protein kinase in skeletal muscle cells. Journal of Cellular Physiology 217, 478–485.
Panel on Antiretroviral Guidelines for Adults and Adolescents. Guidelines for the use of antiretroviral agents in HIV-1-infected adults and adolescents, 2008. Department of Health and Human Services. November 3, 2008, pp. 1–139.
Ranganathan, S., Kern, P.A., 2002. The HIV protease inhibitor saquinavir impairs lipid metabolism and glucose transport in cultured adipocytes. Journal of Endocrinology 172, 155–162.
Richmond, S., Carper, M.J., Lei, X., Zhang, S., Yarasheski, K., Ramanadham, S., 2010. HIV-protease inhibitors suppress skeletal muscle fatty acid oxidation by reducing CD36 and CPT1 fatty acid transporters. Biochimica et Biophysica Acta 1801, 559–566.
Rudich, A., Vanounou, S., Riesenberg, K., Porat, M., Tirosh, A., Harman-Boehm, I., Greenberg, A.S., Schlaeffer, F., Bashan, N., 2001. The HIV protease inhibitor Nelfinavir induces insulin resistance and increases basal lipolysis in 3T3-L1 adipocytes. Diabetes 50, 1425–1431.
Sevastianova, K., Sutinen, J., Kannisto, K., Hamsten, A., Ristola, M., Yki-Järvinen, H., 2008. Adipose tissue inflammation and liver fat in patients with highly active antiretroviral therapy-associated lipodystrophy. American Journal of Physiology. Endocrinology and Metabolism 295, E85–E91.
Shoelson, S.E., Lee, J., Goldfine, A.B., 2006. Inflammation and insulin resistance. Journal of Clinical Investigation 116, 1793–1801.
Shulman, G.I., 2000. Cellular mechanisms of insulin resistance. Journal of Clinical Investigation 106, 171–176.
Solinas, G., Naugler, W., Galimi, F., Lee, M.-S., Karin, M., 2006. Saturated fatty acids inhibit induction of insulin gene transcription by JNK-mediated phosphorylation of insulin-receptor substrates. PNAS 103, 16454–16459.
Torriani, M., Thomas, B.J., Barlow, R.B., Librizzi, J., Dolan, S., Grinspoon, S., 2006. Increased intramyocellular lipid accumulation in HIV-infected women with fat redistribution. Journal of Applied Physiology 100, 609–614.
Wang, Y., Zhao, Z., Li, Y., Li, Y., Wu, J., Fan, X., Yang, P., 2010. Up-regulated α-actin expression is associated with cell adhesion ability in 3-D cultured myotubes subjected to mechanical stimulation. Molecular and Cellular Biochemistry 338, 175–181.
Xu, X., Zhao, X., Liu, T.C., Pan, H., 2008. Low-intensity laser irradiation improves the mitochondrial dysfunction of C2C12 induced by electrical stimulation. Photomedicine and Laser Surgery 26, 197–202.
Zhang, Q., Wu, D., Han, D., Zhang, G., 2007. Critical role of PTEN in the coupling between PI3K/AKT and JNK1/2 signaling in ischemic brain injury. FEBS Letters 581, 495–505.